A Journal of the Gesellschaft Deutscher Chemiker

Angewandte International Edition GDCh Chemie

www.angewandte.org

Accepted Article

Title: A Light-controllable Chemical Modulation of m6A RNA Methylation

Authors: Ling Lan, Ying-Jie Sun, Xiao-Yang Jin, Li-Jun Xie, Li Liu, and Liang Cheng

To be cited as: *Angew. Chem. Int. Ed.* 10.1002/anie.202103854

Link to VoR: https://doi.org/10.1002/anie.202103854

WILEY-VCH

10.1002/anie.202103854

RESEARCH ARTICLE

WILEY-VCH

A Light-controllable Chemical Modulation of m^{6}A RNA Methylation

Ling Lan,[a][c] Ying-Jie Sun,[a][c] Xiao-Yang Jin,[a][c] Li-Jun Xie,[a] Li Liu[a][c] and Liang Cheng*[a][b][c]

Dedicate to Prof. emeritus Dong Wang on the occasion of his 80th birthday.

[a] L. Lan, Y.-J. Sun, X.-Y. Jin, Dr. L.-J. Xie, Prof. L. Liu and Prof. L. Cheng
Beijing National Laboratory for Molecular Sciences (BNLMS), CAS Key Laboratory of Molecular Recognition and Function, CAS Research/Education Center for Excellence in Molecular Sciences, Institute of Chemistry, Chinese Academy of Sciences
Beijing 100190, China
E-mail: chengl@iccas.ac.cn
[b] Prof. L. Cheng
Hangzhou Institute for Advanced Study, University of Chinese Academy of Sciences
Hangzhou 310024, China
[c] L. Lan, Y.-J. Sun, X.-Y. Jin, Prof. L. Liu and Prof. L. Cheng
University of Chinese Academy of Sciences
Beijing 100049, China.

Supporting information for this article is given via a link at the end of the document.

Abstract: Bioactive small molecules with photo-removable protecting groups have provided spatial and temporal control of corresponding biological effects. Herein we presented the design, synthesis, computational and experimental evaluation of the first photo-activatable small-molecule methyltransferase agonist. By blocking the functional N-H group on MPCH with a photo-removable *ortho*-nitrobenzyl moiety, we have developed a promising photo-caged compound that had completely concealed its biological activity. Short UV light exposure of cells treated with that caged molecule in a few minutes resulted in a considerable hypermethylation of m^{6}A modification in transcriptome RNAs, implicating a rapid release of the parent active compound. This study validates for the first time the photo-activatable small organic molecular concept in the field of RNA epigenetic research, which represents a novel tool in spatiotemporal and cellular modulation approaches.

Introduction

Till now, over 170 post-transcriptional RNA epigenetic modifications have been identified on a variety of RNAs, including mRNA, tRNA, rRNA, lncRNA, miRNA, snoRNA and other non-coding RNAs.[1] Similar to that highly diverse distribution, the functions of those epigenetics varied significantly in diverse physiological processes, such as genetic information translation and regulation processes.[2] Their abnormal change have been shown in the association with a plethora of human disease.[3] Thus, a precise regulation of a particular RNA variant is highly desirable. Indeed, classical genetic approaches such as knockouts/downs, mutations, and overexpression of corresponding RNA-modifying enzymes (RMEs) have led to the discovery of several significant molecular mechanisms behind those epigenetic marks.[1a, 4] Furthermore, the development of chemical tools targeting those RMEs have attracted considerable attention in the last decade.[5] However, an efficient approach to manipulate a particular modification in cellular environment with high a spatiotemporal precision is still a challenge.

N^6-Methyladensoine m^{6}A is one the most abundant internal modifications in mRNAs, presenting in 1~4‰ of all adenosines in global cellular RNAs.[6] Dysregulated m^{6}A methylation levels has been proven to affect RNA metabolism and hence lead to various diseases.[7] For example, a decrease of m^{6}A caused by amplified demethylase activity contributed to the onset of obesity,[8] while increased levels of m^{6}A methylation were associated with the progression of human abdominal aortic aneurysm[9] and human brain developing.[10] Therefore, considerable progress has been made in the discovery and development of methyltransferase/demethylase-based organic molecules for cancer therapy.[11] Despite these advances, our understanding of intracellular functionalities of m^{6}A is inadequate by the lack of approaches allowing for a selective modulation of this methylation process with high spatial and temporal precision. Non-invasive manipulation of cellular processes by light-activated biomacromolecules and chemical probes has recently developed as an emerging scientific field.[12] However, being able to control RNA epigenetics with spatiotemporal control still represented a challenge. More recently, we have demonstrated an *in vitro* artificial demethylation of m^{6}A through flavin mononucleotide facilitated biocompatible photo-oxidation[13] and a small molecular triggered deprenylation of cytokinins in live plant *Arabidopsis thaliana*.[14] In this report, we demonstrated that a photo-responsive chemical method is feasible for a precise spatiotemporal modulation of particular RNA modification, m^{6}A for example, in live cells (Scheme 1A).

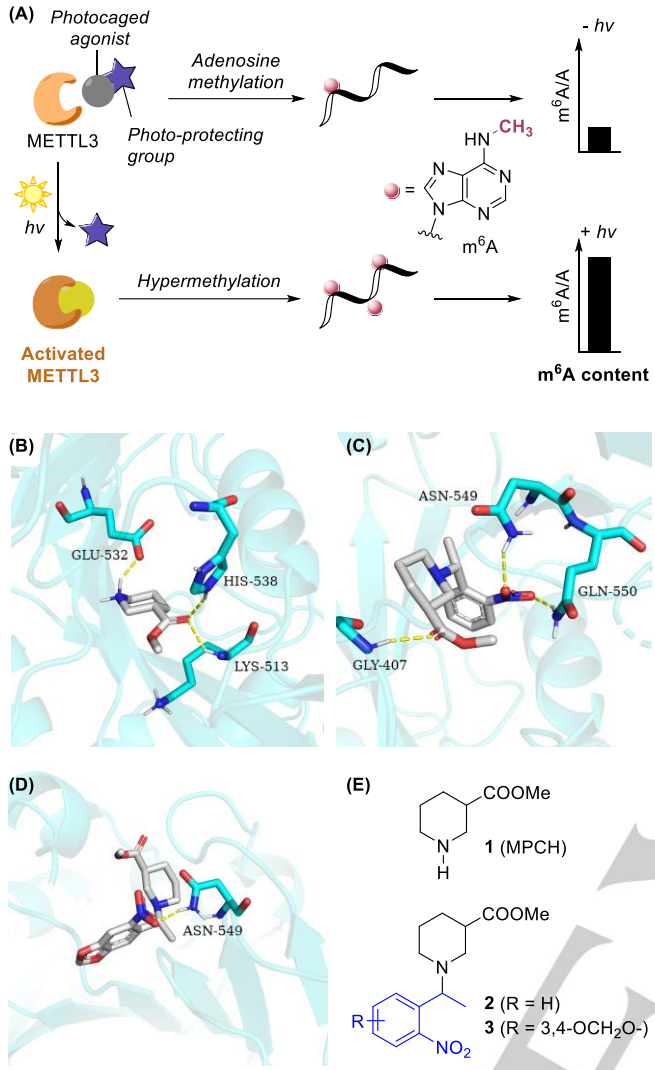

Scheme 1. (A) Concept of a light-triggered RNA methylation of adenosine promoted by the methyltransferase METTL3. A METTL3 agonist was conjugated with a photo-caging group in the active site that blocked its binding. The methylation underwent without interruption, yielding a normal m^{6}A level. Irradiation with light (*hv*) removes the caging group, releasing the compound and activating METTL3, resulting in higher m^{6}A methylation level. (B) The docking model and the interaction diagram with the lowest energy of METTL3/14 complex with compound **1** (as shown in (E)). The yellow dashed lines were used to indicate the key hydrogen bonds between the two molecules. (C) The docking model and the interaction diagram with the lowest energy of METTL3/14 complex with compound **2** (as shown in (E)). (D) The docking model and the interaction diagram with the lowest energy of METTL3/14 complex with compound **3** (as shown in (E)). (E) Structures of the METTL3 agonist **1** and the caged compounds **2-3**. Blue part represents the photo-caging groups.

Results and Discussion

Given the essential role of methyltransferases in the transferring methyl group from *S*-adenosylmethionine (SAM) to designated RNAs, we sought to achieve a light-regulated control over its function with photo-stimulated small molecules. We exemplify the feasibility of this opto-modulation approach by utilizing a piperidine-3-carboxylate **1** (MPCH, Schemes 1B, E), an organic molecule that was recently identified to activate the triprotein complex METTL3/14/WTAP pertaining to m^{6}A installation.[15] The agonism was believed to arise from multiple cooperative interactions between piperidine ring with surrounding residues in METTL3/14 complex, as established in previous studies. In contrast to traditional approaches by randomly grafting photo-caging groups onto chemical functionalities, we used the computational docking to precisely guide and evaluate the caging strategy. The program AutoDock 4.2 was used to characterize the binding of METTL3/14 complex (PDB: 5K7W) with small compounds (Schemes 1B-D, Tables 1 and S2).[16] It showed that the agonist **1** could preferably occupy a cavity of SAM binding channel in a similar manner with a high affinity by interacting mainly with the Glu^{532} (with N-H), His^{538} and Lys^{513} (both with C=O) residues. The binding energy (ΔG) was calculated as -6.86 kcal·mol^{-1}, while the binding sites were deduced with Lys^{513} and His^{538} (both with the carboxyl group), and Glu^{532} (with the amino group), respectively. These binding results were highly consistent with previous report (ΔG = -6.94 kcal·mol^{-1}, binding at Lys^{513} and Glu^{532}).[15] However, we also observed some other binding modes other than at the SAM channel (for other inferior binding modes and their interacting sites, see *Supporting Information* for details). These allosteric binding effects should be taken into consideration when high concentration of small organic molecules are used.[15] We anticipated that a simple and yet appropriate *N*-caging group would not only obstruct the key interaction with Glu^{532}, but would also impede other favorable bonding by inducing a large conformational change of the chair-like structure of the piperidine. We thus designed two masked compounds bearing 2-nitrophenyl methyl ethyl (**2**) and [4,5]dioxole substituted (**3**) photo-caging substituents at the key N-H (Scheme 1E) and calculated their binding affinities with METTL3/14 complex (Schemes 1C-D, Table 1). We did observe significant changes in their structures, which caused the disappearance of all crucial interactions embedding in the METTL3/14-SAM-binding channel.[17] On the other hand, some trivial contacts with surrounding residues were detected (Table 1), which suggested that the entire large size molecules produced differential interactions, which were consistent with their much lower binding energies (ΔG = -5.56 and -6.24 kcal·mol^{-1}, respectively), dissociation constants (K_i = 83.95 and 26.79 μM, respectively) and ligand efficiencies (LE = 0.26) comparing with compound **1** (K_i = 9.43 μM and LE = -0.69). Thus, the temporal concealing of N-H and the relatively large substituents would make it possible to be a brake on the compound binding with METTL3 and thus totally block its agonism. Transcriptome RNAs would then be methylated without interruption and yielding a normal m^{6}A amount. If the caging group were removed upon light exposure to release their precursor that would then subsequently activate METTL3, a higher m^{6}A methylation level would be accomplished. Therefore, the molecular docking suggested it provide an efficient means to modulate the corresponding methyltransferase activity and regulate the m^{6}A RNA level without RMEs engineering.

Table 1. Thermodynamic parameters for the binding interactions between METTL3/14 and three small molecules **1-3** by molecular docking calculations[a]

	ΔG (kcal·mol^{-1})	K_i (μM, 298K)	Ligand efficiency (LE)	H-bond(s)[b]
1	-6.86	9.43	-0.69	Lys^{513} (-C=O) His^{538} (-C=O)

				Glu^{532} (-NH_2^+)
2	-5.56	83.95	-0.26	Gln^{550} (-NO_2) Asn^{549} (-NO_2) Gly^{407} (-C=O)
3	-6.24	26.79	-0.26	Asn^{549} (-NO_2)

[a] Full calculations and predictions performed with AutoDock 4.2 was listed in Table S2. [b] Main bindings between the METTL3/14 complexes with the small molecules **1-3**. Surrounding amino acid residues and their corresponding interacting chemical functionalities within the small molecules (in parentheses) were listed.

Based on our model, we synthesized two masked agonists **2**-**3** by introducing 2-nitrophenyl methyl ethyl and [4,5]dioxole substituted photo-caging substituents onto the key N-H (Schemes 1E). This was achieved by employing a regioselective and efficient alkylation with appropriate 2-nitrobenzyl bromides (See *Supporting Information* for details). Simpler 2-nitrobenzyl protecting groups (R' = H) were not utilized (Scheme 2A).[18] Although they have been proven to be good photo-removable groups for aliphatic amines, the generated 2-nitroso benzaldehydes **4** (R' = H) upon photolysis may condense with the release amine to form imine byproducts and thus hamper the biological activity restoration. In contrast, 2-nitroso acetophenones like **5** (R' = Me) would reduce the risk of those side effects (Scheme 2A). To determine the profiles and kinetics of the photo-responsive release, we measured the photolytic characterization of these compounds (Schemes 2B-C). UV spectra of compounds **1-3** (Scheme 2B) revealed that precursor **1** showed no absorption at 230-500 nm range, whereas the photo-caged **2** possessed a characteristic absorption around 262 nm and the dioxole moiety in **3** shifted the characteristic absorption to around 356 nm. In order to examine the photo-dissociation speediness, we used a light-emitting diode (LED) reactor at a wavelength of 365 nm (100 mW·cm^{-2}) to irradiate compounds **2-3** (200 μM). Mass spectra and UV analysis of samples collected over a period of 5 minutes confirmed that agonist **1** was smoothly released under this condition, with the generation of corresponding 2-nitroso acetophenones **5**[19] as revealed by UV absorbance (Schemes 2C-D, Figures S1-S2). Furthermore, after 2 minutes of irradiation, approximately 80% of the bioactive antagonist **1** was regenerated from compound **2**, and the maximum restoration was reached within 5 minutes of irradiation (k_{obs} = 6.45 × 10^{-3} s^{-1}, $t_{1/2}$ = 106.6 s). Previous reports have indicated that electron-rich substituted 2-nitrobenzyl groups like [4,5]dioxolyl **3** usually photolyzed more efficiently than its unsubstituted counterpart.[20] Conversely, a lower uncaging efficiency of photolysis of **3** was observed in our case, with the reaction progress curve reached plateau after 10 minutes (k_{obs} = 2.61 × 10^{-3} s^{-1}, $t_{1/2}$ = 265.5 s) (Scheme 2C). The reason for the decreased performance of dioxole substituent was not clear. In the photo-caging concept, it is essential that the parent molecule be speedily released by light exposure. Otherwise, a long-time irradiation would cause DNA damage along with the photo-caging group cleavage. Thus, those data confirmed that caged compound **2** possessed excellent uncaging kinetics and was then chosen for enzymatic and *in vitro* investigations.

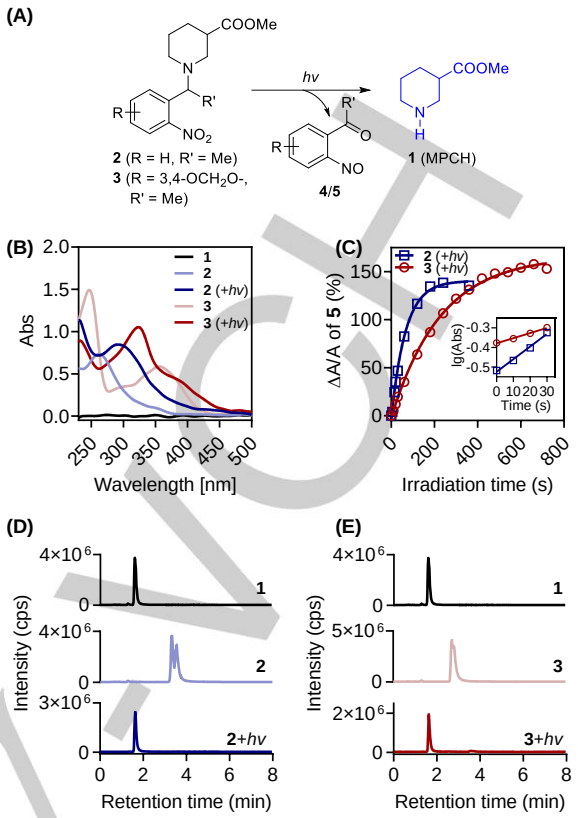

Scheme 2. (A) Photo-induced de-caging reaction of compounds **2-3**. (B) UV-vis absorption spectra of compounds **1-2** at 200 μM and compound **3** at 150 μM in DMSO/H_2O (v/v 1/1000) before and after light irradiation (λ = 365 nm, 100 mW·cm^{-2}). Black line: **1** without *hv* irradiation. Ice blue: compound **2** before light irradiation. Navy blue: compound **2** under light irradiation after 5 minutes. Salmon: compound **3** before light irradiation. Maroon: compound **3** under light irradiation after 10 minutes. (C) Time course for photo-induced uncaging of **2** (navy blue) and **3** (maroon) at λ = 365 nm. The Y axial corresponds to the absorbance change of generated nitrosoketones. The calculation is detailed in the SI materials. (Data collected at λ = 262 nm for **2** and 356 nm for **3**, respectively). Inset: Determination of the initial rate constants (k_{obs}) for the photo-deprotection of compounds **2** (navy blue) and **3** (maroon). (D) Liquid chromatography mass spectrometry (LC-MS) total ion current (TIC) diagram of the photo-deprotection reaction of caged compounds **2**. Black: compound **1**. Ice blue: compound **2** before light irradiation. Navy blue: compound **2** under light irradiation after 5 minutes. The new peak was identical to compound **1** according to the retention time. (E) LC-MS (TIC diagram) of the photo-deprotection reaction of caged compounds **3**. Black: compound **1**. Salmon: compound **3** before light irradiation. Maroon: compound **3** under light irradiation after 10 minutes. The new peak was identical to compound **1** according to the retention time.

To further assess the inactivity of caged compound **2**, as well as its reactivation ability upon light exposure, we performed a bioluminescence-based assay to measure the activities of methyltransferases METTL3/14 under the modulation of small molecules **1** and **2** (Scheme 3). During the transmethylation reaction of adenosine to m^{6}A, the methyl donor SAM was converted to a more stable and yet uncharged byproduct *S*-adenosyl homocysteine (SAH) accompanied by the release of methylated RNA from METTL3/14-RNA complex. In this assay, we incubated the METTL3/14 complex with appropriate RNA substrates and compounds **1** or **2** and then hydrolyzed the key by-product SAH to homocysteine and adenine. The latter was phosphorylated to afford adenosine triphosphate (ATP), and was

then quantified using the classical luciferase reaction. Thus, the methyltransferases activity (m^6A generation) was quantified by the luminescence output (Scheme 3A). Two ssRNAs 5'-UACACUCGAUCUGGACUAAAGCUGCUC-3' and 5'-CUGGACUGGACUGG'-3' containing one and two m^6A consensus motifs (GGACU) respectively, were used in this assay (Underlined letter A indicated the methylation position). We first validated the luminescence signal by utilizing the agonist **1** (Figure S4). In that case of ssRNA with two motifs, an increase of luminescence signal ($\Delta\Delta_{SAH\%}$ = 46.5%) was observed at 1 nM concentration of **1**, clearly indicating that the enzymes were fully and functionally activated (Figures S5-S6). As expected, the caged compound **2** did not cause any significant change in dark conditions, which was consistent with its relatively weak binding affinity as determined before (Table 1) and again indicated that the *N*-photocaging sufficiently suppressed the agonism effect. However, its activation was efficiently reinstated after exposure to the 365 nm light (100 $mW{\cdot}cm^{-2}$) within as short as 5 minutes ($\Delta\Delta_{SAH\%}$ = 43.7%). The renovated activity of **2** was approximately comparable to the original compound **1**, therefore confirming its photo-responsive activity (Scheme 3B). Thus, the rapid uncaging of **2** by light irradiation has enabled the modulation of corresponding methyltransferase METTL3/14 complex activity for m^6A methylation with the same efficacy as the unmodified **1**.

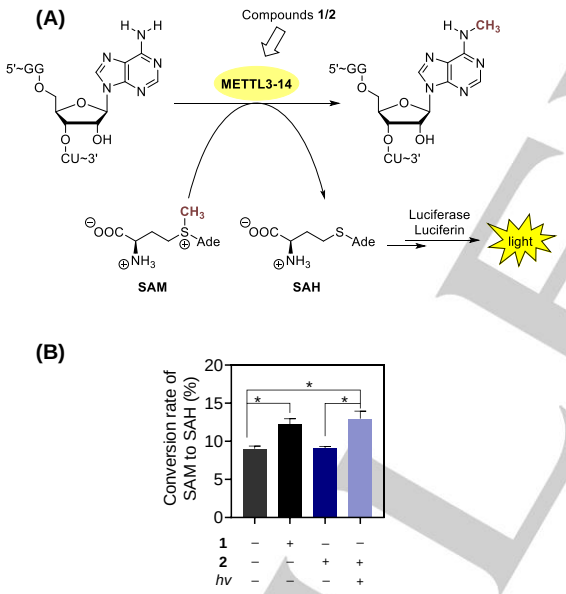

Scheme 3. (A) Bioluminescence-based assay used for the determination of METTL3/14 complex activity on adenosine methylation of two ssRNAs 5'-UACACUCGAUCUGGACUAAAGCUGCUC-3' and 5'-CUGGACUGGACUGG'-3' upon treatment with small compounds **1** and **2** with or without light irradiation (Underlined letter A indicated the methylation position). The by-product SAH was used as the luminescence trigger for detection. (B) The effects of photo-caged small molecule for the METTL3/14 complex on the RNA substrate methylation using enzymatic assay in (A). The Y axial corresponds to the ratio of SAH generated from the original SAM (1 μM), and the calculation is detailed in the *Supporting Information*. Error bars indicate mean ± SEM (n = 3~6), normalized to DMSO-treated samples for each sample. Unpaired students' *t* test. $*p < 0.05$.

Having established such an effective approach to disrupt the METTL3 agonism, we next investigated whether the adjustable performance of compound **2** upon light irradiation could be used to differentially modulate the m^6A methylation in live cells, and thus allow us to spatially and temporally investigate the epigenetic effects in biological events (Scheme 4). We tested three different cell lines: A549, MCF-7 and HeLa. As expected, no change was observed after exposure to compounds **1** or **2** (100 nM) in HeLa cell line with or without light irradiation, confirming that the light-activation manipulation strategy together with the developed small organic molecules had no statically significant effect on the cell viability (Figure S7). With a concentration of both molecules **1** and **2** at 1 nM, which matched to the amount used in previous enzymatic experiments with greatest activity (Figure S8), RNA dot blot analysis[21] demonstrated that cells incubated with caged compound **2** without light irradiation failed to exhibit significant m^6A methylation increase compared with the control groups, suggesting that the installation of photo-caging groups completely detached its activity and also the caged compound has negligible side-effects to the live cells (Scheme 4B, Figure S9). Consistently, 5 minutes of light irradiation revealed that mRNAs within cells incubated with compound **2** were considerably hyper-methylated when compared to other intervention groups (control and without irradiation). Of note, comparable levels of m^6A with **2** under light irradiation have been observed for all three cell lines compared to those treated with unmodified **1** (Scheme 4B, Figure S9). In order to exclude other possible effect factors of regulating m^6A level, we identified the target METTL3 and METTL14 proteins with western blot from HeLa cells incubated with compounds **1** and **2**, with or without light irradiation (Figure S10). The expression of METTL3/14 was determined before and after chemical treatment and irradiation treatments, and the results clearly proved that there is no side-effect on the corresponding m^6A methyltransferases' expression. Taken together, these results not only supported previous enzymatic analysis showing the agonist effects could be predominately removed by introducing a photo-caging group, but also suggested that the caged compound **2** is particularly stable for potential therapeutic utilization in living organisms, in which it can be promptly initiated by light irradiation in the needing time and place without genetic approaches.

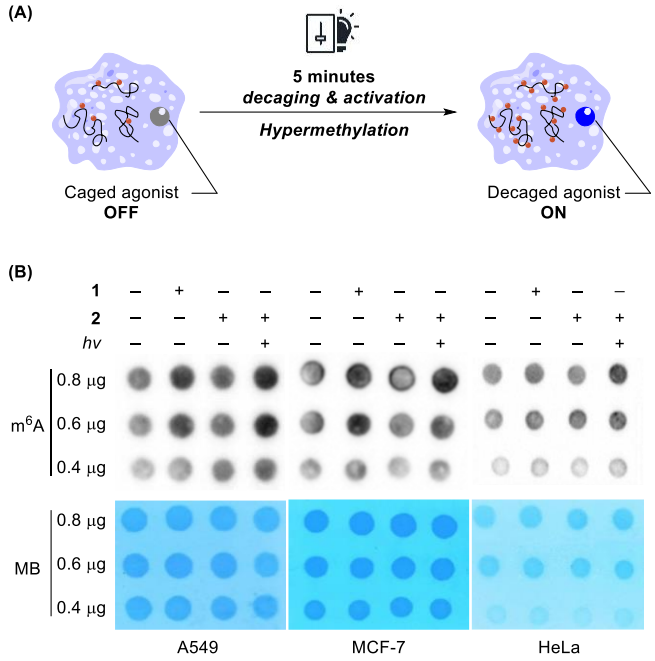

Scheme 4. (A) Schemic demontrstation of this chemical approach in controlling METTL3/14 complex function with light to modulate the m^{6}A RNA methylation status in live cells. Red circles represent m^{6}A modification. Gray ball (within the left) represents compound **2**, which upon light irradiation was converted to **1** (blue ball, within the right). (B) Determination of m^{6}A abundance in the three human cancer cell lines upon **1** or **2** (1 nM for A549 and HeLa, 100 nM for MCF-7) treatment for 4 hours by dot blot assay. The RNA loading amount is from 0.8 μg to 0.4 μg. Cells upon treatment with **2** after 2 hours incubation were irradiated for 5 minuts (365 nm, 100 mW·cm^{-2}). A methylene blue staining (MB) was used as loading control.

Conclusion

Stimuli-responsive chemical probes that target RMEs involved in RNA epigenetic modification are powerful techniques for controlling their activities. Their application to modulate RNA modification processes *in vitro* or *in vivo*, especially during embryonic development, might provide an effective tool to understand the complication of this epitranscriptomic regulatory system. Additionally, these methods can also be cherished as excellent starting points for developing novel drugs against several diseases such as cancers and viral infections pertaining to RNA modification dysregulation. However, to the best of our knowledge, such stimuli-gated chemical molecules for epitranscriptomic modulation of intracellular processes like m^{6}A methylation has not been realized yet. Here, we have developed a novel chemical modular for m^{6}A based on a photo-caging strategy with the agonist compound MPCH **1**. Molecular docking of this molecule helped propose binding modes within the methyl donor SAM-binding sites of METTL3 and helped guide the photo-caging substituents identified in this work, which is one of the main perspectives of this work. Our synthesized compound **2** showed little binding affinity and activation effects against the m^{6}A methyltransferase complex METTL3/14 in dark. Importantly, we observed a clear gain-of-function in the biochemical assay and live human cancer cells upon light exposure, which significantly altered the cellular m^{6}A levels. It is expected that the observed effects are produced by the extremely rapid photo-decaging to release the precursor compound. In addition, since the decaging/activation process occurred with fast dynamics (< 5 minutes), ultraviolet radiation caused cytotoxicity is reduced to minimal. On the other hand, the opto-control system that we used is based on the chemical agonist of methyltransferases, which is principally suitable for utilization in living systems, as it can be swiftly initiated by light irradiation, without the requirement of addition/deletion of endogenous enzymes. This may be useful in the case of dealing with other epigenetic marks. Since the caging groups can be easily changed, it would be a useful starting point to expand to other caged ligands with miscellaneous chemical properties to be installed during the preparation step followed by stimuli-activation. For example, by combining two or more chemical components (agonist and/or inhibitors) into an assembly that is covalently linked by a photo-caging group, one can achieve an efficient dual modulation of multiple RMEs simultaneously with appropriate light-irradiation. It fuses the gains of photo-responsive chemical tools in terms of flexibility without protein engineering[22] and the distinguish activities (*i.e.*, both activation and inhibition of function) can be evoked respectively. This approach might be, therefore, an excellent technique to precisely modulate RNA modification for the control of cell activities.

Acknowledgements

This work was supported by the National Key R&D Program of China (2016YFA0602900, 2017YFA0208100, and 2020YFA0707901), National Natural Science Foundation of China (22022704, 91853124, 21977097, and 21778057) and Chinese Academy of Sciences. Dr. L.-J. Xie is supported by the Postdoctoral Innovative Talents Support Program (BX20200337). We thank Prof. Cai-Guang Yang, Dr. Yue Huang at Shanghai Institute of Materia Medica, CAS and Prof. Xia Dong from Institute of Chemistry, CAS for insightful discussions and help with dot-blot experiments.

Keywords: RNA modification • Epigenetics • Small organic agonist • Photo-decaging • Spatiotemporal control

[1] a) H. Shi, J. Wei, C. He, *Mol. Cell* **2019**, *74*, 640-650; b) P. Boccaletto, M. A. Machnicka, E. Purta, P. Piątkowski, B. Bagiński, T. K. Wirecki, V. de Crécy-Lagard, R. Ross, P. A. Limbach, A. Kotter, M. Helm, J. M. Bujnicki, *Nucleic Acids Res.* **2018**, *46*, D303-D307; c) N. Liu, T. Pan, *Nat. Struct. Mol. Biol.* **2016**, *23*, 98-102.

[2] a) I. A. Roundtree, M. E. Evans, T. Pan, C. He, *Cell* **2017**, *169*, 1187-1200; b) W. V. Gilbert, T. A. Bell, C. Schaening, *Science* **2016**, *352*, 1408; c) I. A. Roundtree, C. He, *Curr. Opin. Chem. Biol.* **2016**, *30*, 46-51; d) A. G. Torres, E. Batlle, L. Ribas de Pouplana, *Trends Mol. Med.* **2014**, *20*, 306-314; e) Y. Saletore, K. Meyer, J. Korlach, I. D. Vilfan, S. Jaffrey, C. E. Mason, *Genome Biol.* **2012**, *13*, 175; f) G. Walsh, R. Jefferis, *Nat. Biotechnol.* **2006**, *24*, 1241-1252.

[3] a) D. C. Henshall, *Eur. J. Paediatr. Neuro.* **2020**, *24*, 30-34; b) R. A. Copeland, M. E. Solomon, V. M. Richon, *Nat. Rev. Drug Discov.* **2009**, *8*, 724-732.

[4] a) P. A. Boriack-Sjodin, S. Ribich, R. A. Copeland, *Nat. Rev. Drug Discov.* **2018**, *17*, 435-453; b) A. Gallo, D. Vukic, D. Michalík, M. A. O'Connell, L. P. Keegan, *Hum. Genet.* **2017**, *136*, 1265-1278; c) K. Nishikura, *Nat. Rev. Mol. Cell Biol.* **2016**, *17*, 83-96.

[5] a) J. Gu, J. Xu, Q. You, X. Guo, *Eur. J. Med. Chem.* **2020**, *196*, 112325; b) L. J. Xie, L. Liu, L. Cheng, *Biochemistry* **2020**, *59*, 230-239; c) H. Ü. Kaniskan, M. L. Martini, J. Jin, *Chem. Rev.* **2018**, *118*, 989-

1068; d) G.-Q. Lai, L.-L. Zhou, C.-G. Yang, *Chin. J. Chem.* **2020**, *38*, 420-421; e) L.-L. Zhou, C.-G. Yang, *Biochemistry* **2020**, *59*, 125-127; f) M. Cully, *Nat. Rev. Drug Discov.* **2019**, *18*, 892-894.

[6] a) N. Liu, K. I. Zhou, M. Parisien, Q. Dai, L. Diatchenko, T. Pan, *Nucleic Acids Res.* **2017**, *45*, 6051-6063; b) N. Liu, Q. Dai, G. Zheng, C. He, M. Parisien, T. Pan, *Nature* **2015**, *518*, 560-564; c) Y. Fu, D. Dominissini, G. Rechavi, C. He, *Nat. Rev. Genet.* **2014**, *15*, 293-306.

[7] a) K. Asada, A. Bolatkan, K. Takasawa, M. Komatsu, S. Kaneko, R. Hamamoto, *Biomolecules* **2020**, *10*, 1071; b) Z. Zhang, K. Luo, Z. Zou, M. Qiu, J. Tian, L. Sieh, H. Shi, Y. Zou, G. Wang, J. Morrison, A. C. Zhu, M. Qiao, Z. Li, M. Stephens, X. He, C. He, *Nat. Genet.* **2020**, *52*, 939-949; c) X. Wang, Z. Lu, A. Gomez, G. C. Hon, Y. Yue, D. Han, Y. Fu, M. Parisien, Q. Dai, G. Jia, B. Ren, T. Pan, C. He, *Nature* **2014**, *505*, 117-120.

[8] X. Zhao, Y. Yang, B. F. Sun, Y. Shi, X. Yang, W. Xiao, Y. J. Hao, X. L. Ping, Y. S. Chen, W. J. Wang, K. X. Jin, X. Wang, C. M. Huang, Y. Fu, X. M. Ge, S. H. Song, H. S. Jeong, H. Yanagisawa, Y. Niu, G. F. Jia, W. Wu, W. M. Tong, A. Okamoto, C. He, J. M. R. Danielsen, X. J. Wang, Y. G. Yang, *Cell Res.* **2014**, *24*, 1403-1419.

[9] Y. He, J. Xing, S. Wang, S. Xin, Y. Han, J. Zhang, *Ann. Transl. Med.* **2019**, *7*, 797.

[10] K.-J. Yoon, F. R. Ringeling, C. Vissers, F. Jacob, M. Pokrass, D. Jimenez-Cyrus, Y. Su, N.-S. Kim, Y. Zhu, L. Zheng, S. Kim, X. Wang, L. C. Doré, P. Jin, S. Regot, X. Zhuang, S. Canzar, C. He, G.-l. Ming, H. Song, *Cell* **2017**, *171*, 877-889.e817.

[11] S. Schwartz, M. R. Mumbach, M. Jovanovic, T. Wang, K. Maciag, G. G. Bushkin, P. Mertins, D. Ter-Ovanesyan, N. Habib, D. Cacchiarelli, N. E. Sanjana, E. Freinkman, M. E. Pacold, R. Satija, T. S. Mikkelsen, N. Hacohen, F. Zhang, S. A. Carr, E. S. Lander, A. Regev, *Cell Rep*. **2014**, *8*, 284-296.

[12] a) Y. Wu, Z. Yang, Y. Lu, *Curr. Opin. Chem. Biol.* **2020**, *57*, 95-104; b) M. M. Dcona, K. Mitra, M. C. T. Hartman, *RSC Med. Chem.* **2020**, *11*, 982-1002; c) N. Ankenbruck, T. Courtney, Y. Naro, A. Deiters, *Angew Chem. Int. Ed.* **2018**, *57*, 2768-2798.

[13] a) L.-J. Xie, X.-T. Yang, R.-L. Wang, H.-P. Cheng, Z.-Y. Li, L. Liu, L. Mao, M. Wang, L. Cheng, *Angew. Chem. Int. Ed.* **2019**, *58*, 5028-5032; b) L.-J. Xie, R.-L. Wang, D. Wang, L. Liu, L. Cheng, *Chem. Commun.* **2017**, *53*, 10734-10737.

[14] H.-P. Cheng, X.-H. Yang, L. Lan, L.-J. Xie, C. Chen, C. Liu, J. Chu, Z.-Y. Li, L. Liu, T.-Q. Zhang, D.-Q. Luo, L. Cheng, *Angew. Chem. Int. Ed.* **2020**, *59*, 10645-10650.

[15] S. Selberg, D. Blokhina, M. Aatonen, P. Koivisto, A. Siltanen, E. Mervaala, E. Kankuri, M. Karelson, *Cell Rep.* **2019**, *26*, 3762-3771 e3765.

[16] a) S. P. Leelananda, S. Lindert, *Beilstein J. Org. Chem.* **2016**, *12*, 2694-2718; b) M. Schapira, *ACS Chem. Biol.* **2016**, *11*, 575-582.

[17] a) P. Śledź, M. Jinek, *elife* **2016**, *5*, 1-16; b) P. Wang, Katelyn A. Doxtader, Y. Nam, *Mol. Cell* **2016**, *63*, 306-317; c) X. Wang, J. Feng, Y. Xue, Z. Guan, D. Zhang, Z. Liu, Z. Gong, Q. Wang, J. Huang, C. Tang, T. Zou, P. Yin, *Nature* **2016**, *534*, 575-578.

[18] C. I. Wendell, M. J. Boyd, *Tetrahedron Lett.* **2015**, *56*, 897-899.

[19] M. Gaplovsky, Y. V. Il'ichev, Y. Kamdzhilov, S. V. Kombarova, M. Mac, M. A. Schwörer, J. Wirz, *Photoch. Photobio. Sci.* **2005**, *4*, 33-42.

[20] a) J. Luo, J. Torres-Kolbus, J. Liu, A. Deiters, *ChemBioChem* **2017**, *18*, 1442-1447; b) P. Klan, T. Solomek, C. G. Bochet, A. Blanc, R. Givens, M. Rubina, V. Popik, A. Kostikov, J. Wirz, *Chem. Rev.* **2013**, *113*, 119-191.

[21] T. Chen, Y. J. Hao, Y. Zhang, M. M. Li, M. Wang, W. Han, Y. Wu, Y. Lv, J. Hao, L. Wang, A. Li, Y. Yang, K. X. Jin, X. Zhao, Y. Li, X. L. Ping, W. Y. Lai, L. G. Wu, G. Jiang, H. L. Wang, L. Sang, X. J. Wang, Y. G. Yang, Q. Zhou, *Cell Stem Cell* **2015**, *16*, 289-301.

[22] A. P. Pelliccioli, J. Wirz, *Photoch. Photobio. Sci.* **2002**, *1*, 441-458.

10.1002/anie.202103854

Entry for the Table of Contents

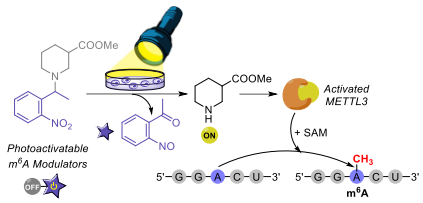

This work demonstrated a novel route for the spatiotemporal control of intracellular RNA epigenetic modifications. The agonism effect of a small compound can be concealed through appropriate photo-responsive caging groups, and the synthesized compounds exhibited a high sensitivity of external light irradiation and rapidly restored their effects in live cells.